Neuron, Vol. 21, 545–559, September, 1998, Copyright ©1998 by Cell Press

Cell Type and Pathway Dependence of Synaptic AMPA Receptor Number and Variability in the Hippocampus

Zoltan Nusser,* Rafael Lujan,† Gregor Laube,‡ J. David B. Roberts, Elek Molnar,§ and Peter Somogyi
Medical Research Council
Anatomical Neuropharmacology Unit
Department of Pharmacology
University of Oxford
Mansfield Road
Oxford OX1 3TH
United Kingdom

Summary

It has been suggested that some glutamatergic synapses lack functional AMPA receptors. We used quantitative immunogold localization to determine the number and variability of synaptic AMPA receptors in the rat hippocampus. Three classes of synapses show distinct patterns of AMPA receptor content. Mossy fiber synapses on CA3 pyramidal spines and synapses on GABAergic interneurons are all immunopositive, have less variability, and contain 4 times as many AMPA receptors as synapses made by Schaffer collaterals on CA1 pyramidal spines and by commissural/associational (C/A) terminals on CA3 pyramidal spines. Up to 17% of synapses in the latter two connections are immunonegative. After calibrating the immunosignal (1 gold = 2.3 functional receptors) at mossy synapses of a 17-day-old rat, we estimate that the AMPA receptor content of C/A synapses on CA3 pyramidal spines ranges from <3 to 140. A similar range is found in adult Schaffer collateral and C/A synapses.

Introduction

Neuronal communication in the cerebral cortex depends, to a large extent, on the properties of glutamatergic synaptic neurotransmission, which have been extensively studied in stratum radiatum of the hippocampal CA1 area. In this region, the origins of pre- and postsynaptic elements are relatively homogeneous; the vast majority of glutamate-releasing presynaptic terminals originate from axon collaterals of pyramidal cells situated in the CA3 area, and they form synapses mostly with dendritic spines of CA1 pyramidal cells. In spite of their uniform origin, individual synaptic junctions show great heterogeneity. There is a wide range in structural parameters, such as the area of the synaptic membrane specialization, the length and volume of dendritic spines, the extent of the spine apparatus, and the number of docked synaptic vesicles (Andersen et al., 1966; Harris and Kater, 1994; Moser et al., 1997; Schikorski and Stevens, 1997; Sorra and Harris, 1998). Furthermore, a wide range in the functional parameters of these synapses has also been described. The transmitter release probability and the readily releasable neurotransmitter pool size of presynaptic Schaffer collateral terminals were found to be heterogeneous (Dobrunz and Stevens, 1997). In addition, the size of the postsynaptic responses at different sites also exhibits variability. This variability may be so extreme that some synapses may contain more than 150 (Jack et al., 1994), whereas others may not have any functional α-amino-3-hydroxy-5-methyl-4-isoxazolepropionate (AMPA) receptors (Kullmann, 1994; Isaac et al., 1995; Liao et al., 1995; Durand et al., 1996). The latter synapses have been named "silent" after experiments showing that, at hyperpolarized potentials, no fast postsynaptic response could be detected, although from the same stimulus site, when the postsynaptic neuron was depolarized, N-methyl-D-aspartate (NMDA) receptor–mediated postsynaptic responses could be observed (Isaac et al., 1995; Liao et al., 1995; Durand et al., 1996). These results were interpreted as evidence for synapses containing functional NMDA receptors without detectable, functional AMPA receptors, a possibility suggested earlier (Kullmann, 1994). However, alternative interpretations of the above results, which do not invoke the absence of functional AMPA receptors at some synapses, have also been put forward (Kullmann et al., 1996; Kullmann and Asztely, 1998).

Whether every glutamatergic synapse contains AMPA receptors, or a significant proportion of synapses lack these receptors, not only has important consequences for neuronal development and plasticity but also has a profound influence on the computational power of a network. Therefore, in order to define the number and variability of AMPA receptors within distinct populations of synapses, we applied a quantitative immunogold localization method. This method has been successfully used to compare the receptor content of distinct synapse populations (Nusser et al., 1994, 1996; Popratiloff et al., 1996; Shigemoto et al., 1996; Landsent et al., 1997; Rubio and Wenthold, 1997) and for examining the variability in the receptor content of a single synapse population (Nusser et al., 1997). A previous study of the CA1 area (Baude et al., 1995) showed a variability in AMPA receptor immunolabeling; synapses on large spines and GABAergic interneuron dendrites were more strongly labeled than those on small spines. As the labeling efficacy was low using single sections and subunit-specific antibodies, the possibility that immunonegative synapses contained a significant amount of AMPA receptors could not be excluded. In order to detect immunoreactivity for all AMPA receptor subunits (GluR1–GluR4) expressed in the hippocampus (Hollmann et al., 1989; Sommer et al., 1990; Rogers et al., 1991; Petralia and Wenthold, 1992; Martin et al., 1993; Molnar et al., 1993; Sato et al., 1993; Baude et al., 1995), we developed

*Present address: Department of Neurology, University of California School of Medicine, Los Angeles, California 90095.
†Present address: Instituto de Neurociencias, Universidad Miguel Hernandez, Facultad de Medicina, Campus de San Juan, 03550 Alicante, Spain.
‡Present address: Institut fur Molekularbiologie und Medizinische Chemie, Universitatsklinikum, Leipziger Strasse 44, D-39120 Magdeburg, Federal Republic of Germany.
§Present address: Department of Pharmacological Sciences, University of Newcastle Upon Tyne, Framlington Place, Newcastle NE2 4HH, United Kingdom.

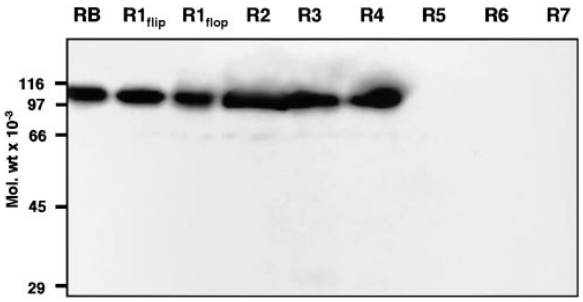

Figure 1. Characterization of the Subunit Specificity of ab-pan-AMPA on Western Blots

Membrane proteins (30 μg/lane) from rat brain (RB) and transiently transfected COS7 cells expressing GluR1–GluR7 subunits were immunostained with the ab-pan-AMPA (1 μg/ml). The ab-pan-AMPA labels a single band at ~110 kDa on rat brain preparation and recognizes all AMPA-preferring subunits (GluR1–GluR4; and both "flip" and "flop" alternatively spliced isoforms) with approximately equal intensity. The kainate-preferring subunits (GluR5–GluR7) are not recognized by the antibody.

a polyclonal antibody recognizing epitope(s) common to all four AMPA-type glutamate receptor (GluR) subunits. Furthermore, to determine the immunoreactive receptor content of the entire postsynaptic area and thus monitor variability due to differences in the size of synapses (Harris and Kater, 1994), serially sectioned synapses were immunoreacted and analyzed.

Results

In previous studies (Petralia and Wenthold, 1992; Martin et al., 1993; Molnar et al., 1993; Baude et al., 1995), the localization of AMPA receptors in the hippocampus was made with antibodies selective for either the GluR1, GluR2/3, or GluR4 subunits. None of the antibodies, on its own, recognizes all AMPA receptor subunits expressed by hippocampal pyramidal cells. Accordingly, if a synapse, for example, is found to be immunonegative for the GluR2/3 subunits, it is still possible that it could contain either GluR1 or GluR4 subunits, making the estimate of immunonegative synapse population unreliable. The antibody (ab-pan-AMPA) developed for this study recognized all four AMPA receptor subunits with approximately equal potency on immunoblot but none of the kainate or NMDA receptor subunits (Figure 1). To estimate the immunoreactive receptor content of the entire postsynaptic area, we serially sectioned stratum radiatum of the Lowicryl resin–embedded CA1 region and reacted each section with the ab-pan-AMPA. The vast majority of the spines in stratum radiatum arise from pyramidal cells; therefore, we will refer to them as pyramidal cell spines. Dendritic shafts receiving several asymmetrical synapses are considered to originate from interneurons. The overwhelming majority of boutons in the CA1 radiatum forming asymmetrical synapses are from contra- (commissural) and ipsilateral (Schaffer collateral) CA3 pyramidal cells; therefore, we refer to them as Schaffer collateral terminals.

In ab-pan-AMPA–reacted sections, many synapses made by Schaffer collateral terminals on spines of adult rat hippocampus contained a large number of gold particles, but others were immunonegative. The strongly immunopositive synapses were consistently labeled on serial sections, and often immunonegativity of a synapse was also consistent. The distribution of Schaffer collateral synapses with regard to their GluR1–GluR4 subunit content was skewed toward larger values (Figure 3A; $p < 0.001$, Shapiro–Wilk test), with a mean number of particles per synapse of 4.9 ± 6.2 (mean $\pm$ SD; range, 0–33; $n = 163$). Approximately 20% of the Schaffer collateral synapses were immunonegative in these reactions. Reacting the same block under identical conditions with an antibody to the GluR2/3 subunits (ab-GluR2/3), a very similar pattern of labeling was observed. The most strongly labeled synapses contained up to 27 gold particles (mean $= 4.4 \pm 5.1$; range, 0–27; $n = 114$), but others were immunonegative. The distribution of GluR2/3 subunit immunoreactivity in Schaffer collateral synapses was also skewed ($p < 0.001$, Shapiro–Wilk test), with ~18% of the synapses being negative. The shape of the distributions obtained with ab-pan-AMPA and ab-GluR2/3 did not differ significantly from one another ($p > 0.05$, Kolmogorov–Smirnov test).

As the interpretation of the immunonegative synapses depends on the sensitivity of our method, we tried to increase the labeling intensity further by applying a mixture of ab-GluR2/3 and ab-pan-AMPA. It was expected that the signal obtained with this mixture could be stronger than that provided by either of the antibodies alone, because the ab-GluR2/3 and the ab-pan-AMPA recognize different epitopes, residues 850–862 (intracellular) and 724–781 (extracellular), respectively, on opposite sides of the plasma membrane. The labeling pattern with the mixture of antibodies was indistinguishable from that obtained with either of the single antibodies, but the strongly positive synapses contained even more immunoparticles. Strongly immunopositive synapses could be observed alongside weakly positive and negative synapses, and this pattern of labeling was consistent through serial sections (Figure 2). The distribution of synapses with regard to their AMPA receptor content was skewed (Figure 3B; $p < 0.001$, Shapiro–Wilk test; rat-1: mean $= 7.6 \pm 9.7$; range, 0–51; $n = 285$; rat-2: mean $= 7.6 \pm 11.5$; range, 0–87; $n = 454$). The very skewed distribution of Schaffer collateral synapses indicated that these synapses do not form a homogenous population. Approximately 14% of Schaffer collateral synapses are immunonegative for AMPA receptor subunits (Figure 4A), ~67% contain between 1 and 10 gold particles (mean $= 4.2 \pm 2.7$), and ~19% have more than 10 particles (mean $= 24.8 \pm 14.3$; range, 11–87). To examine whether the large variability in the immunoparticle number is a consequence of the variability in the size of synapses as it has been found at GABAergic synapses (Nusser et al., 1997), we reconstructed the membrane specialization of Schaffer collateral synapses from serial sections. A significant positive correlation between the gold particle number and the size of synapses was found (Figure 4B), suggesting a similar receptor density between different synapses. However, the variability in the gold particle number (coefficient of variation [CV] = SD/mean; rat-1, 1.25; rat-2, 1.45) was larger than the variation in the synaptic area (CV: rat-1, 0.60; rat-2, 0.56), indicating that receptor density is also variable between synapses. When the immunoparticle density was examined as a function of synaptic area (Figure 4C), a larger variability was found in small than in large synapses.

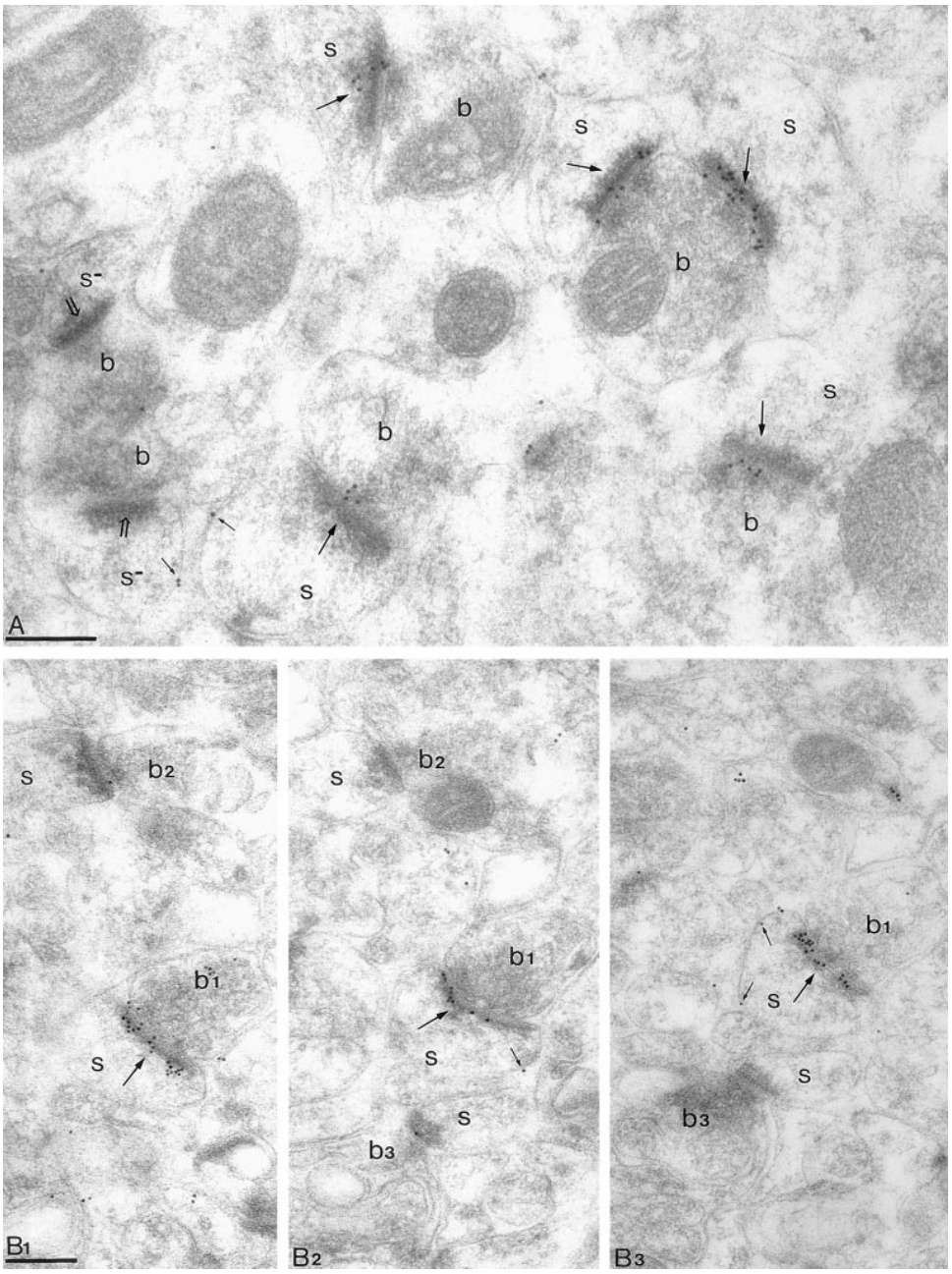

Figure 2. Large Variability in the AMPA Receptor Content of Schaffer Collateral Synapses on Spines of CA1 Pyramidal Cells in Stratum Radiatum

(A) Asymmetrical synapses made by boutons (b) with spines (s) may contain a large number of (arrows) or no (open arrows in s^-) immunoparticles for AMPA receptor subunits (ab-pan-AMPA + ab-GluR2/3).

(B_1–B_3) Serial sections showing the consistency of labeling from section to section. The large synapse (arrow) made by a terminal (b_1) with a spine (s) is strongly immunopositive, whereas other synapses (b_2 to s and b_3 to s) on smaller spines contain either one particle or no particles in serial sections. Large spines are also consistently labeled on the extrasynaptic membrane (small arrows in [A] and [B]). Scale bars, 0.2 μm.

Is this distribution of receptor content unique to the Schaffer collateral synapses, or is it a general feature of all classes of cortical glutamatergic synapses exhibiting distinct functional properties? Strata lucidum and radiatum of the CA3 area include commissural/associational (C/A) synapses on spines of pyramidal cells, C/A synapses on GABAergic interneurons, and mossy fiber synapses on complex spines of pyramidal cells. We used the mixture of the ab-pan-AMPA and ab-GluR2/3 on serial sections of Unicryl resin–embedded adult rat hippocampus to determine the immunoreactive AMPA receptor content of these three distinct populations of glutamatergic synapses. The labeling pattern for AMPA receptor subunits in the stratum radiatum of the CA3 area was indistinguishable from that in the stratum radiatum of the CA1 area. Strongly immunopositive synapses were found alongside immunonegative ones, and the labeling or the lack of it was consistent in serial

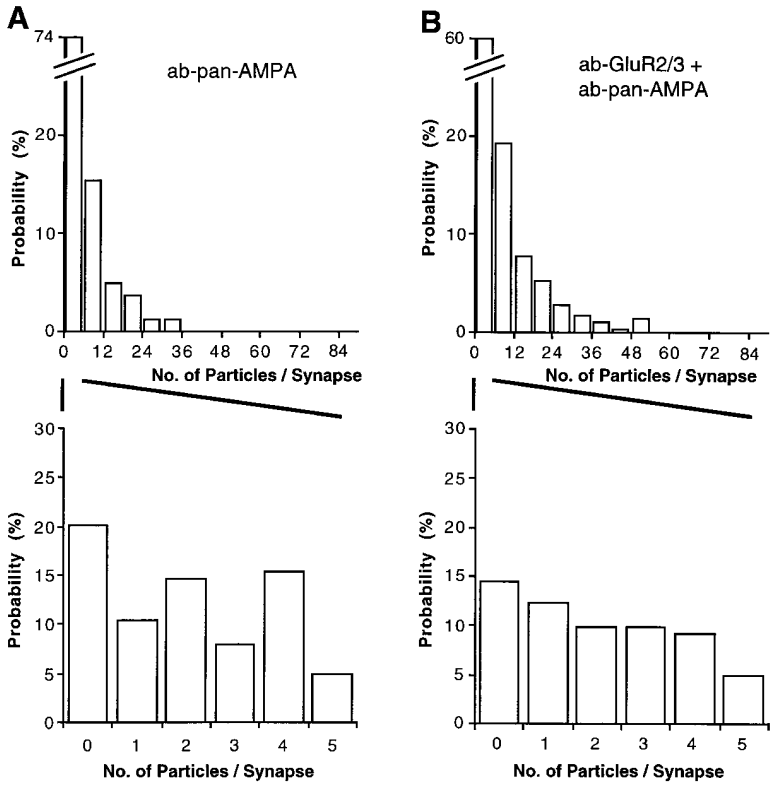

Figure 3. Large Variability in Receptor Number at Synapses on CA1 Pyramidal Cell Spines

The distribution of synapses according to their immunoreactive AMPA receptor content is skewed toward larger values as revealed by immunogold reactions either with ab-pan-AMPA alone ([A]; rat-1: mean ± SD = 4.9 ± 6.2 particles per synapse; n = 163 synapses) or with the mixture of ab-GluR2/3 and ab-pan-AMPA ([B]; rat-1: 7.6 ± 9.7 particles per synapse; n = 285). Bottom panels show the rebinned data of the first bin of the distributions. Although the highest number of gold particles per synapse was 51 with the antibody mixture in this animal, ~15% of the synapses remained immunonegative.

sections (Figure 5). Immunonegative and strongly positive synapses were found to be established by two release sites of a single bouton on different spines (e.g., Figure 5), demonstrating that presynaptic activity alone cannot be responsible for the amount of expressed AMPA receptors. The distribution of AMPA receptors in these synapses (rat-A: mean = 4.7 ± 8.8; range, 0–59; n = 182) also resembled that of Schaffer collateral synapses. The relationship between the area and immunoparticle content of C/A synapses was very similar to that of Schaffer collateral synapses in the CA1 area, with more variable immunoparticle density at small synapses. In an additional animal (rat-B), we succeeded in increasing further the efficiency of labeling, which is reflected in a higher mean (9.6 ± 19.8; n = 91) and maximum (94) number of particles per synapse. In spite of this, the shape and the CV (1.9 [rat-A] versus 2.1 [rat-B]) of the distributions from the two rats remained very similar. Different sensitivity obtained in the two animals (rat-A and rat-B) may be due to different fixation conditions and/or different antigen preservations during slam-freezing, freeze-substitution, and low-temperature embedding. Although the mean and maximum number of particles per synapse was 104% and 59% higher, respectively, in rat-B, the proportion of immunonegative synapses (rat-A, 17.0%; rat-B, 16.5%) remained virtually the same. If the immunonegative synapses contained a significant number of receptors, one would expect that increasing the sensitivity by 2-fold would result in the approximate halving of the immunonegative synapse population. The lack of change in the proportion of immunonegative synapses therefore supports the notion that immunonegativity indeed represents a lack of receptors in the synaptic junctions.

The dendrites of GABAergic interneurons are distributed throughout the hippocampal layers and receive synaptic inputs from Schaffer and commissural collaterals, which also innervate the pyramidal cell spines. This provides an opportunity to compare the receptor distribution in synapses of distinct cell types innervated by a common afferent, in order to test the influence of the postsynaptic cell on receptor expression. Every asymmetrical synapse on dendritic shafts of interneurons was immunopositive for AMPA receptor subunits (Figure 6). As a consequence of the consistent, strong labeling and the lack of immunonegative synapses, on average, these synapses contained ~3.5 times as many gold particles (rat-A: mean = 14.8 ± 6.7; range, 4–26; n = 17; rat-B: mean = 38.1 ± 22.5; range, 2–96; n = 31) as C/A synapses on spines in the CA3 area (Figure 8A). This consistent immunopositivity of asymmetrical synapses on GABAergic interneurons was also observed in stratum radiatum of the CA1 area. The mean number of particles per synapse (rat-1: mean = 24.9 ± 18.7; range, 9–76; n = 12; rat-2: mean = 31.7 ± 13.5; range, 10–58; n = 22) was ~4 times higher in synapses made by Schaffer collateral terminals with interneurons than with pyramidal spines. The subunit composition of AMPA receptors in interneuron synapses may not be the same as in pyramidal cells, and this could possibly contribute to the difference in the number of immunoparticles per synapse between the two cell types. The distributions of interneuron synapses with respect to their AMPA receptor content in the CA1 and CA3 areas were not significantly different from normal ($p > 0.05$, Shapiro–Wilk test). Hence, characteristic differences between the distribution of AMPA receptors in interneuron dendritic shaft versus pyramidal spine synapses include the lack

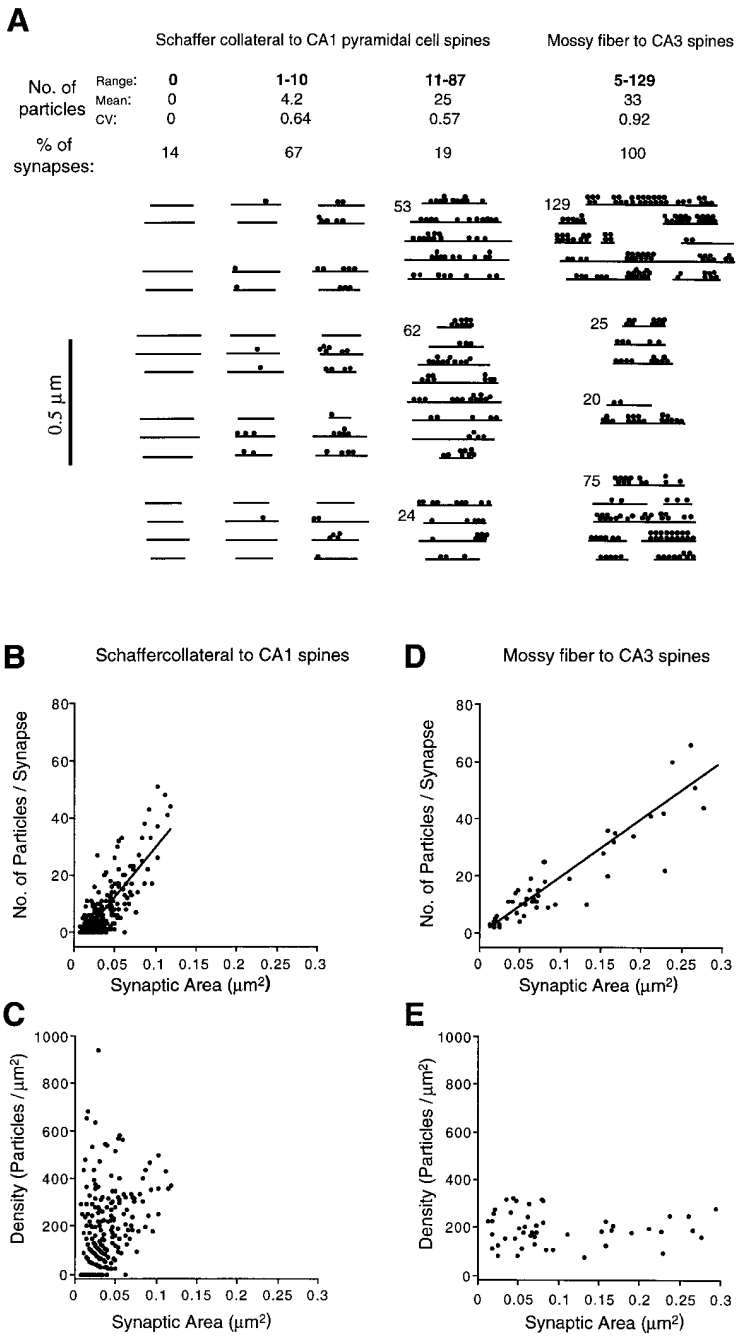

Figure 4. Immunoparticle Density at Schaffer Collateral and Mossy Fiber Synapses

(A) En face view of serially reconstructed synapses with solid lines indicating the sectioned synaptic junctional membranes separated by 75 nm (thickness of the sections). Gold particles are illustrated by dots. Schaffer collateral synapses have been arbitrarily grouped into three categories, and several examples are shown for comparison. Approximately 14% of the Schaffer collateral synapses are immunonegative for AMPA receptor subunits, ~67% contain between 1 and 10 gold particles, and ~19% have more than 10 particles (mean and CV are given for each group; pooled data from two rats). Note that synapses of similar size can be immunonegative or may contain up to 10 particles. Mossy fiber to CA3 pyramidal cell synapses also vary in size, but all of them are immunopositive in each section.

(B) There is a significant positive correlation ($p < 0.01$, Spearman rank correlation; slope of regression line = 345 gold/μm^2; $r = 0.79$; $n = 249$ [rat-1]) between the size and immunoparticle content of Schaffer collateral synapses.

(C) Immunoparticle density shows large variability that is more pronounced in small than in large synapses (same synapses as in [B]).

(D) There is a similar correlation between the size and gold particle content of mossy synapses ($p < 0.01$, Spearman rank correlation) to that of Schaffer collateral synapses, but the slope of the regression line is lower (202 gold/μm^2; $r = 0.91$; $n = 49$ [rat-A]).

(E) The variability in the immunoparticle density is much less in mossy than in Schaffer collateral synapses. Note that the size of mossy synapses is larger than that of Schaffer collateral synapses.

of immunonegative synapses, ~4 times higher gold particle number per synapse, and a much smaller variability (interneurons, CV = 0.55 ± 0.15; spines, CV = 1.68 ± 0.36; pooled from CA1 and CA3 areas) of the interneuron synapses. These results demostrate that the origin of the presynaptic terminal alone cannot be responsible for the number of postsynaptic AMPA receptors.

To investigate to what extent the pattern of AMPA receptor expression is determined by the postsynaptic cell, we compared the distribution of AMPA receptors in two functionally distinct synapses on CA3 pyramidal cells: synapses made by large mossy fiber terminals with complex spines in stratum lucidum and C/A synapses on spines in stratum radiatum. As a complex pyramidal cell spine receives 20–30 asymmetrical synaptic junctions from a large mossy fiber terminal (Chicurel and Harris, 1992), we measured separately the immunoreactive receptor content of each synaptic specialization. Asymmetrical synapses between large mossy fiber terminals and spines always contained gold particles for AMPA receptors (Figures 4 and 7). The average number of particles per mossy synapse was ~4 times as high (rat-A: mean = 18.8 ± 16.2; range, 1–82; n = 56; rat-B: mean = 33.1 ± 30.5; range, 5–129; n = 62) as in C/A synapses on spines (Figure 8A). There was also a difference in the variability of receptor content of mossy

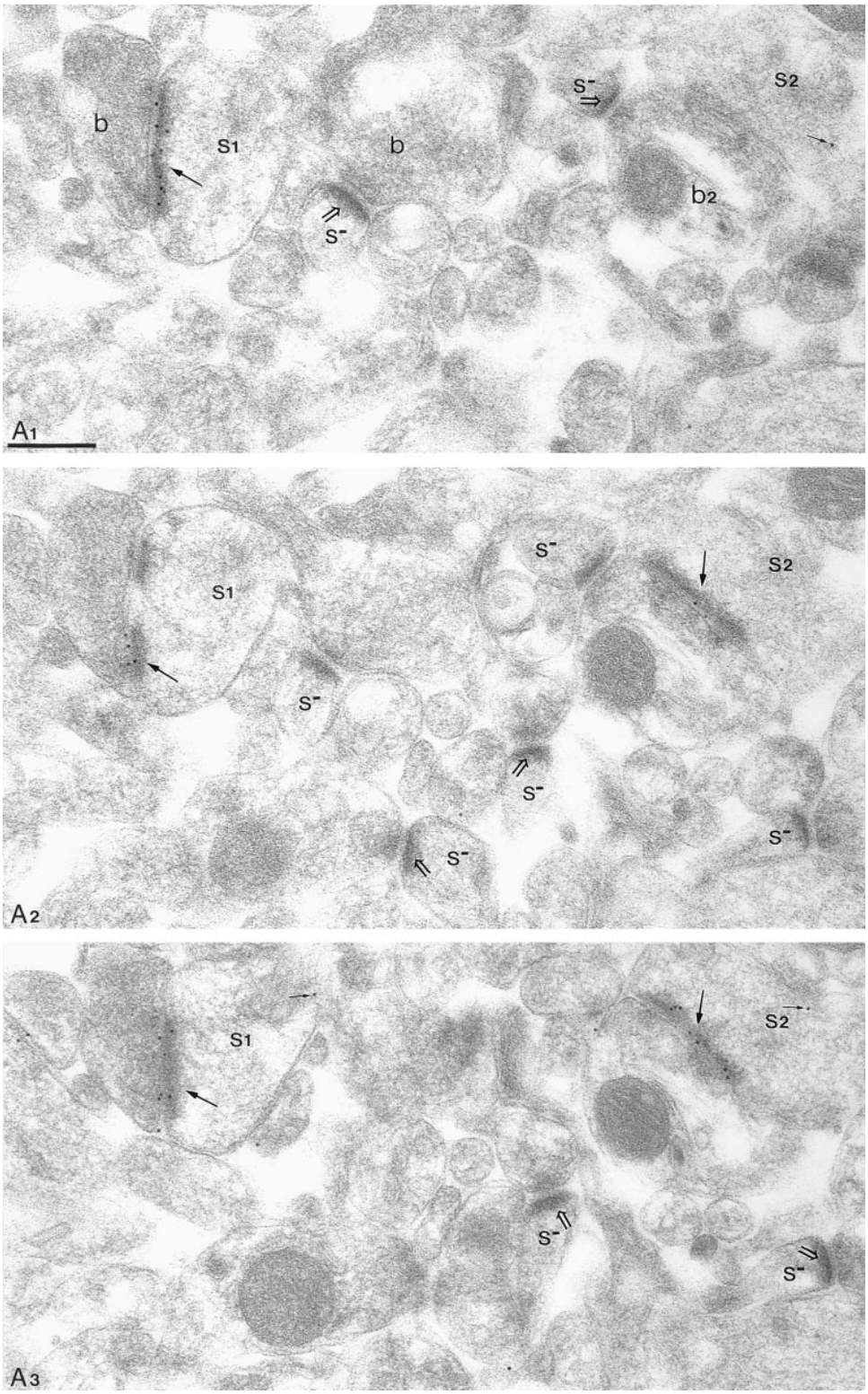

Figure 5. C/A Synapses on CA3 Pyramidal Cell Spines in the Stratum Radiatum Show a Large Variation in Their AMPA Receptor Content

Serial ultrathin sections of the stratum radiatum demonstrate that some synapses (arrows) made by C/A terminals (b) with spines (s_1 and s_2) of pyramidal cells contain a large number of gold particles, whereas other synapses (open arrows) on spines (s^-) are immunonegative (ab-pan-AMPA + ab-GluR2/3). A bouton (b_2) makes two release sites with two spines (s^- and s_2), one of which (open arrow) is immunonegative and is fully shown. The other one (arrow) was present in five serial sections (two are shown) and contained 31 gold particles. Some particles are also present on extrasynaptic spine membranes (small arrows). Scale bar, 0.2 μm.

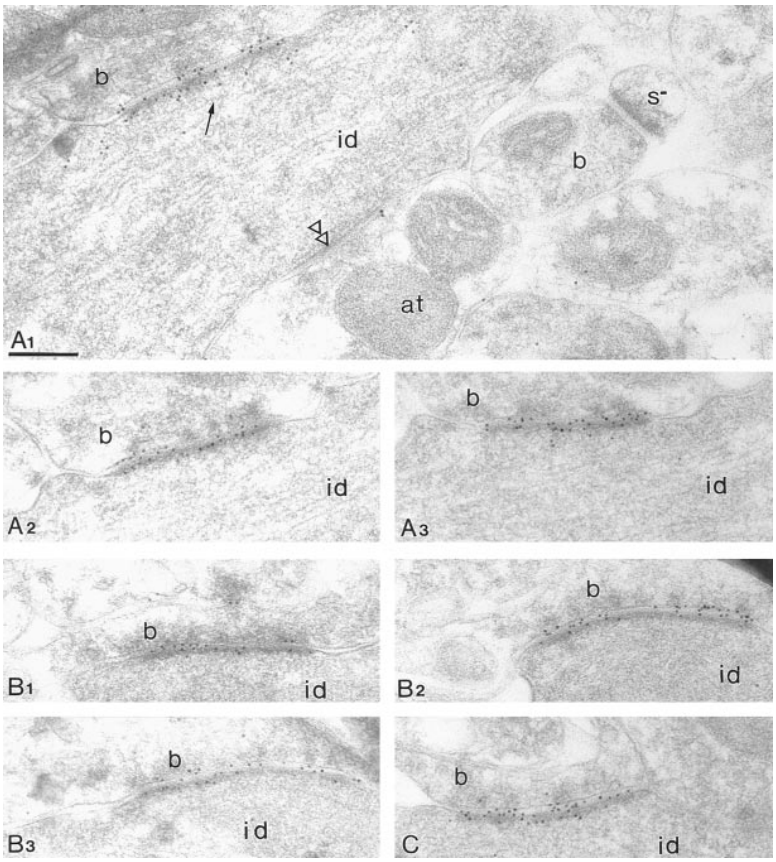

Figure 6. Synapses on GABAergic Interneurons Are Always Strongly Immunopositive for AMPA Receptors (ab-GluR2/3 and ab-pan-AMPA)

A bouton (b in [A_1]) makes a strongly immunopositive asymmetrical synapse (arrow) with the dendritic shaft of an interneuron (id) in the stratum radiatum of the CA3 area. This synapse is shown in two additional serial sections (A_2 and A_3). The same dendrite receives an immunonegative symmetrical synapse (double open triangles) from a presumed GABAergic axon terminal (at). The strong immunolabeling of the interneuron synapse (arrow in [A_1]) is in contrast with the lack of labeling of a synapse between a C/A terminal (b) and a pyramidal cell spine (s^-). Nine asymmetrical synapses were found on this interneuron dendrite (ten serial sections), all of which contained a very large number of gold particles. Two additional interneuron synapses are illustrated in (B) and (C), one of which is shown in three serial sections (B_1–B_3). Scale bar, 0.2 μm.

(rat-A, CV = 0.86; rat-B, CV = 0.92) versus C/A synapses (rat-A, CV = 1.87; rat-B, CV = 2.06), although both synapse populations had a non-Gaussian, skewed distribution. Interestingly, the variability in the gold particle number was similar to the variation in the size of mossy synapses (rat-A, CV = 0.80; rat-B, CV = 0.82). In addition, there was a very significant positive correlation between the size and gold particle content of mossy synapses (Figure 4D), indicating that the receptor density is very similar between synapses. These results suggest that immunoparticle density at mossy synapses has a small variability (Figure 4E), unlike at spine synapses in stratum radiatum. In summary, the distribution of AMPA receptors is remarkably different in two functionally distinct synapse populations on a single cell type (Figure 8). Differences include the lack of immunonegativity, a smaller variability, and ~4 times higher gold particle number of the mossy fiber synapses. Since a single postsynaptic cell can have distinct synapse populations with respect to the AMPA receptor content, it is concluded that factors governing the amount of AMPA receptor in a given glutamatergic synapse are provided by both pre- and postsynaptic elements.

To estimate the number of functional receptors represented, on average, by a single gold particle (scaling factor), we calibrated the immunosignal against functional receptors. Such a calibration would allow us to determine: (1) the number of functional receptors in a given synapse; (2) the smallest, largest, and average number of functional receptors within a synapse population; and (3) the lower limit of immunocytochemically detectable functional receptor number. A possible method of calibration is to determine the number of functional receptors in a homogeneous population of synapses using electrophysiological methods and to measure the immunosignal in the same synapse population (Nusser et al., 1997). Mossy synapses on CA3 pyramidal cells appear to be homogeneous, and Jonas et al. (1993) have estimated the number of functional non-NMDA receptors at mossy synapses on CA3 pyramidal cells of 15- to 24-day-old (P15–P24) Wistar rats. Therefore, we prepared hippocampal tissue from Wistar rats of similar age (P17) and immunoreacted serially sectioned synapses with the mixture of ab-GluR2/3 and ab-pan-AMPA. Serial sections of Unicryl resin–embedded strata lucidum and radiatum of P17 rats showed a very similar pattern of labeling to that obtained in adult rats (cf. Figures 8A and 8B). Although the mean and maximum numbers of particles per C/A synapse on spines of the P17 rat were very similar to those of adult rat-A (P17 rat: mean = 4.6 ± 9.2; range, 0–58; n = 156; versus rat-A: mean = 4.7 ± 8.8; range, 0–59), the proportion of immunonegative synapses was 11% higher in the younger animal (P17 rat, 28%, versus rat-A, 17%). All synapses between mossy fiber terminals and pyramidal cell spines or between C/A terminals and interneuron dendrites were immunopositive. Mossy fiber synapses formed a non-Gaussian, skewed distribution ($p < 0.01$,

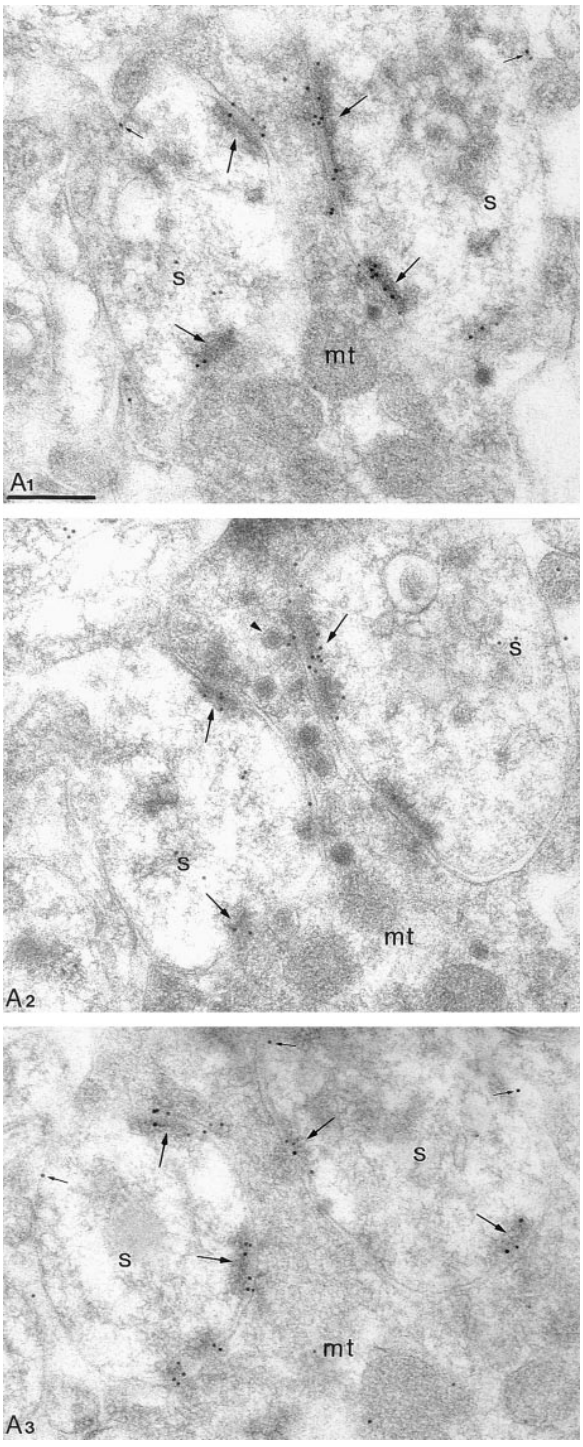

Figure 7. Mossy Fiber Synapses on Spines of CA3 Pyramidal Cells Are Always Immunopositive for AMPA Receptors

Synapses (arrows; ab-GluR2/3 and ab-pan-AMPA) between a mossy fiber terminal (mt) and pyramidal cell spines (s) are shown in serial sections. Mossy fiber terminals contain a large number of synaptic vesicles, several mitochondria, and dense-core vesicles (e.g., arrowhead). Some gold particles are also present on the extrasynaptic spine membranes (small arrows). Scale bar, 0.2 μm.

Shapiro–Wilk test) and contained 35.3 ± 23.3 gold particles (range, 5–89; n = 55), similar to that seen in adult rats (cf. Figures 8A and 8B).

The distribution of tetrodotoxin-resistent, miniature excitatory postsynaptic currents (mEPSCs) of presumed mossy fiber origin is also skewed with a mean of 17.6 pA, corresponding to a mean apparent conductance of 251 pS (Jonas et al., 1993). However, it was estimated that the dendritic cable and the series resistance reduced the peak conductance of mossy fiber EPSCs to 30%–90% of the real value (Jonas et al., 1993). Taking an average of 40% reduction of the real peak conductance, a mean synaptic peak conductance of 418 pS is calculated. As the mean single channel conductance of non-NMDA receptors is 8.5 pS on CA3 pyramidal cells, on average, 49.2 channels open at the peak of the mEPSCs (Jonas et al., 1993). Given a maximum receptor open probability (P_o) of 0.71 and a receptor occupancy of 0.85, on average, 81 functional non-NMDA receptors are calculated to be present in mossy synapses of P15–P24 rats (Jonas et al., 1993), which provides a scaling factor of ~2.3 channels per gold particle (81/35.3). If some of the synaptic AMPA receptors were in a desenzitized state in slice preparation, this would result in a slight underestimation of the scaling factor and the functional receptor number at mossy synapses. However, this uncertainty is smaller than the one originating from the unknown degree of dendritic filtering. A similar calculation can be made by using the quantal size estimate of evoked EPSCs at mossy fiber synapses. Jonas et al. (1993) have found that the average quantal conductance change was 133 pS, which results in a scaling factor of ~1.2. We prefer to use the more conservative estimate of the scaling factor, because the quantal size estimate originates from synapses made by a single mossy fiber terminal with a pyramidal cell. As mEPSCs arise from a larger population of mossy synapses, they contain a larger intersite variability. Our immunogold data are also not restricted to synapses made by a single presynaptic mossy fiber terminal with a pyramidal cell spine and are expected to match the mEPSC distribution better. For these reasons, we can conclude that immunonegative synapses contain less than 3 functional receptors (Figure 8B), but the most strongly immunolabeled synapses may accommodate as many as 210 AMPA receptors.

Immunoreactive AMPA receptors have also been demonstrated to exist in endoplasmic reticulum, Golgi apparatus, multivesicular bodies, and extrasynaptic plasma membranes of several cell types (Petralia and Wenthold, 1992; Martin et al., 1993; Molnar et al., 1993; Baude et al., 1994, 1995; Kharazia et al., 1996). In particular, AMPA receptor immunoreactivity was found in the extrasynaptic spine membrane of hippocampal pyramidal cells with a different immunogold method (Baude et al., 1995). The present study confirmed the immunogold labeling of the extrasynaptic spine membrane with the postembedding method (Figures 2, 5, 7, and 9), and gold particles for AMPA receptors were also detected in the spine apparatus (Figure 9) of some pyramidal cell spines. Immunolabeling in the spine apparatus and extrasynaptic plasma membrane locations were most often present at large spines that received strongly immunopositive synapses (Figure 9). Spines that received small, immunonegative synapses usually did not contain gold particles either in the spine apparatus or in the extrasynaptic plasma membrane. This observation supports the view

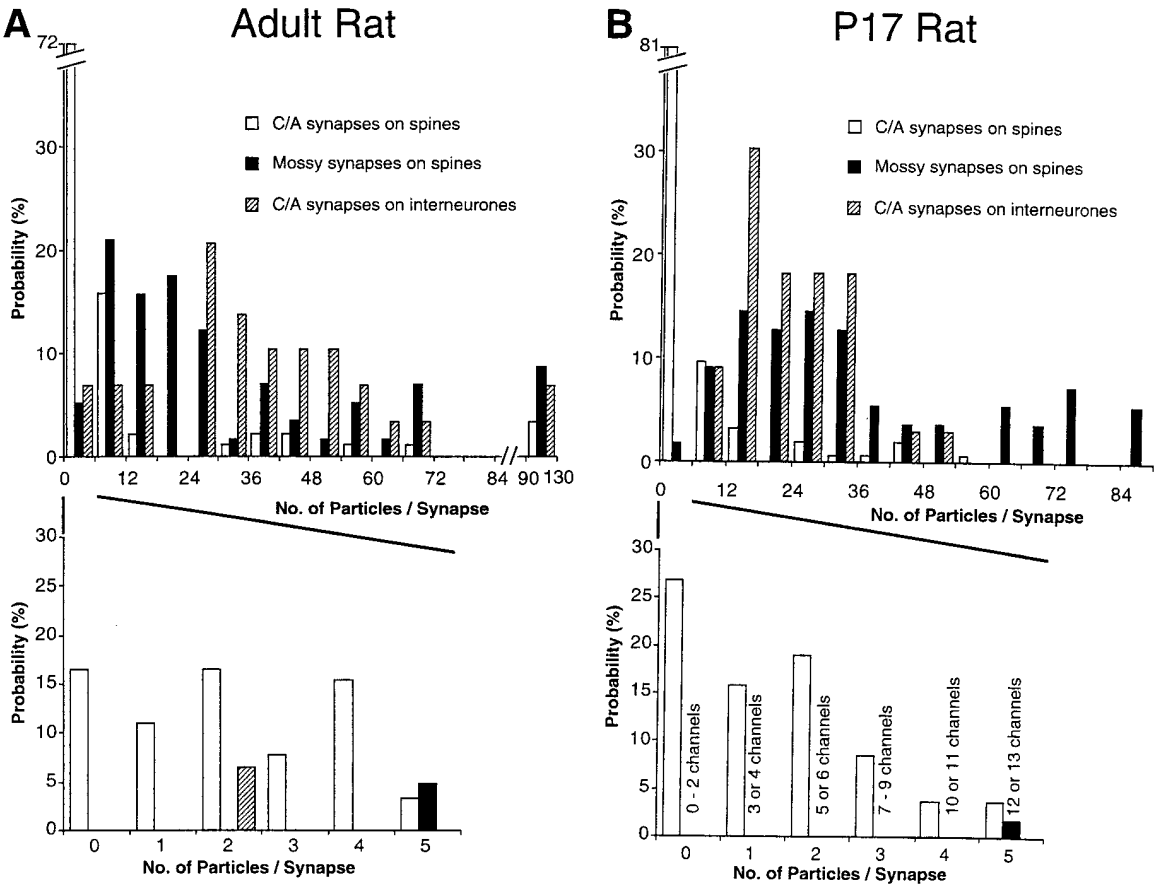

Figure 8. Distribution of AMPA Receptors at Distinct Excitatory Synapses in the CA3 Area of Adult and 17-Day-Old Rats

(A) In adult rats (rat-B shown), the distribution of receptors in C/A synapses on pyramidal cell spines (open columns) is very different from that in C/A synapses on interneurons (striped columns) and in mossy synapses on pyramidal cell spines (closed columns). The distribution of C/A synapses on spines is skewed with a CV of 2.1 (mean = 9.6 ± 19.8; range, 0–94; n = 91). Approximately 16.5% of the synapses are immunonegative as shown in the bottom panel. In stratum radiatum, synapses on GABAergic interneurons contain, on average, ~4 times as many particles (mean = 38.1 ± 22.6; n = 31) as those in spines with a much smaller CV (0.59). As shown in the bottom panel, no immunonegative asymmetrical synapse is found on interneuron dendrites (range, 2–96). Mossy synapses on pyramidal cell spines have a skewed distribution, with a mean number of particles per synapse of 33.1 ± 30.4 (n = 62) and a CV of 0.92. Every mossy synapse is immunopositive for AMPA receptors (range, 5–128).

(B) The distribution of mossy synapses on pyramidal cell spines (closed columns) of a P17 rat hippocampus is remarkably similar to that of the adult rat. The mean number of gold particles per mossy synapse is 35.3 ± 23.3 (CV = 0.66; n = 55), without any synapse being immunonegative (range, 5–89; see bottom panel). Synapses on interneurons (striped columns) in the stratum radiatum have a similar distribution but contain somewhat fewer gold particles in P17 (mean = 22.2 ± 10.4; CV = 0.47; range, 7–49; n = 33) than in adult rats. The distribution of C/A synapses on pyramidal cell spines of a P17 rat is very similar to that of the adult, but it contains 11.5% more immunonegative synapses (28%), and the mean number of particles per synapse is also less (mean = 4.6 ± 9.3; CV = 2.0; range, 0–58; n = 156). The bottom panel shows the rebinned data of the first bin of the distribution and the corresponding number of functional AMPA receptor channels calculated after calibrating the immunosignal (1 gold = 2.3 channels; see Results).

that AMPA receptors in the spine apparatus and in the extrasynaptic plasma membrane represent receptors involved in receptor turnover.

Discussion

Functional Calibration Reveals a High Sensitivity of the Immunogold Localization

It has been shown previously that some of the Schaffer collateral to CA1 pyramidal cell synapses are immunonegative under conditions when others are labeled by several immunogold particles for the GluR1, GluR2/3, or GluR4 subunits of the AMPA-type GluRs (Baude et al., 1995). However, in our previous study the labeling efficacy was low; therefore, the possibility that immunonegative synapses contained a significant number of AMPA receptors could not be excluded. Since then, several developments have lead to an increase in the sensitivity of our immunogold method. These are: (1) the production of an antibody (ab-pan-AMPA), recognizing all subunits of the AMPA-type GluR; (2) coapplication of ab-pan-AMPA and ab-GluR2/3 to maximize receptor recognition; and (3) optimization of the conditions of the reactions. Finally, reactions on completely serially sectioned synapses (Nusser et al., 1997) allow the visualization of the immunoreactive receptor content of the entire postsynaptic area and, therefore, reflect variability due to differences in the size and shape of synapses.

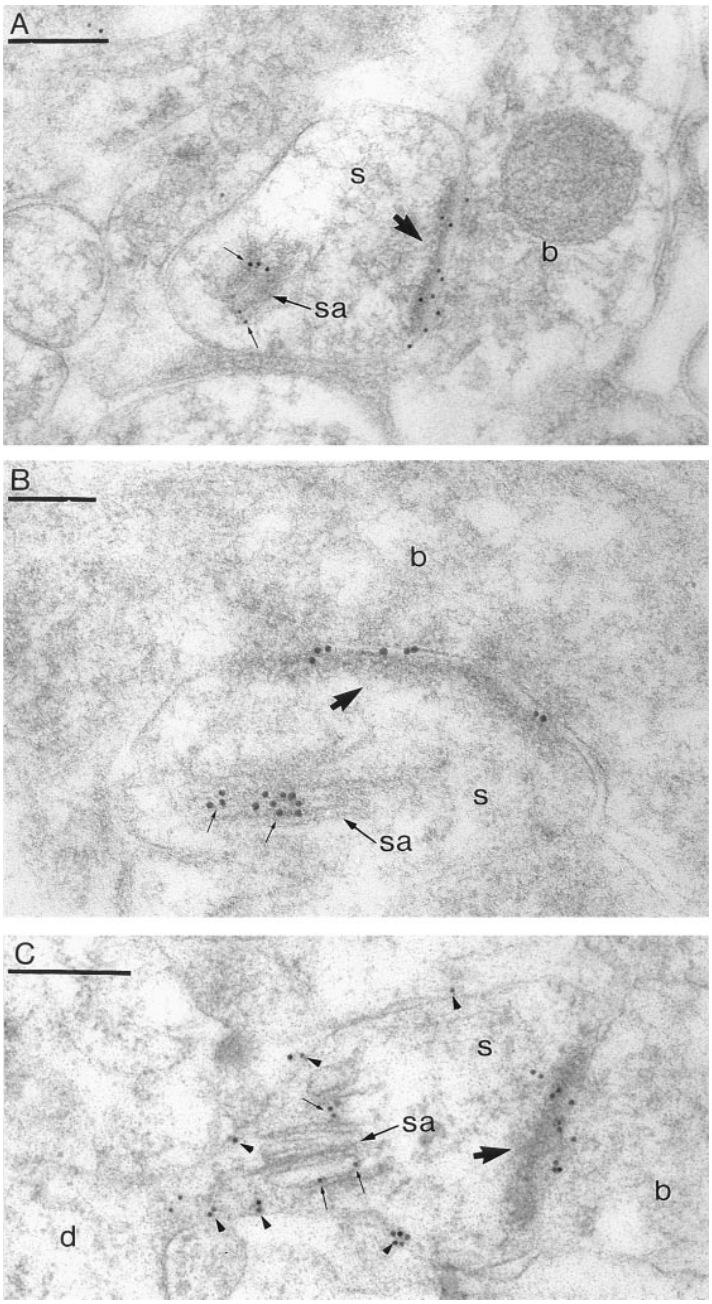

Figure 9. Demonstration of Three Distinct Pools of Immunoreactive AMPA Receptors in Spines of Hippocampal Pyramidal Cells

(A–C) Gold particles are found in the synaptic junctions (large arrows), in the spine apparatus (sa, small arrows) and on the extrasynaptic plasma membranes (arrowheads) of CA3 pyramidal cell spines (s). Immunoparticles in the spine apparatus and in the extrasynaptic plasma membrane location are most often present at large spines that receive a strongly immunopositive synapse. Small immunonegative synapses are usually not labeled in the spine apparatus or in the extrasynaptic membrane. Abbreviations: d, dendrite of a pyramidal cell; b, bouton.

(A) ab-GluR2/3 and ab-pan-AMPA.

(B and C) ab-pan-AMPA.

Scale bars, 0.2 μm (A and C); 0.1 μm (B).

As a result of these developments, the numbers of gold particles detected in a single synapse have become as high as 129, the average number of gold particles in C/A synapses on GABAergic interneurons is 38.1, and mossy synapses on CA3 pyramidal cells and synapses on GABAergic interneurons are all immunopositive in our reactions. In spite of this high labeling efficacy, ~15% and 28% of spine synapses in the stratum radiatum are still immunonegative in adult and P17 rats, respectively.

Our results demonstrate a great variability in the AMPA receptor content of different synapse populations. To estimate the smallest, largest, and average number of functional receptors within a synapse population and the lower limit of immunocytochemically detectable functional receptor number, we had to calibrate the immunosignal against the estimated number of functional receptors in the same synapses. As the estimated mean number of functional non-NMDA receptors at mossy synapses of P15–P25 rats is 81 (see results and Jonas et al., 1993) and the mean number of immunogold particles per synapse in the same population is 35.3, one gold particle represents, on average, 2.3 functional receptors. Accordingly, in P17 rats the lowest and highest numbers of functional receptors in mossy synapses are estimated to be 12 and 205, respectively. Similarly, it is calculated that the number of functional receptors ranges from 16 to 113 with a mean of 50 in glutamatergic synapses on GABAergic interneurons. Taking into account a P_o of 0.6–0.8 (Jonas et al., 1993; Silver et al., 1996; Forti et al., 1997), the opening of 7–13 AMPA receptors is predicted during the smallest EPSCs, which is probably

detectable with somatic recordings. However, in 28% of the C/A synapses on spines in P17 rats, the number of functional receptors is probably less than 3, although the largest synapses contain a similar number of receptors (up to 135) to those on interneurons. Therefore, the synaptic currents generated in a significant proportion of dendritic spines may not be detectable due to the lack of or low AMPA receptor content.

Synapses without Detectable AMPA Receptors

The presence of so-called "silent" glutamatergic synapses in the hippocampus and neocortex has been proposed by several studies on the basis of in vitro electrophysiological experiments (Kullmann, 1994; Isaac et al., 1995, 1997; Liao et al., 1995; Durand et al., 1996). One possibility put forward stipulates that AMPA receptors are present at all synapses, but at some synapses they are in a nonfunctional form. Alternatively, they may not be present at all in some synaptic junctions (Richmond et al., 1996). Our results, providing direct evidence for the presence of a significant population of synapses on spines in the stratum radiatum with less than 3 functional AMPA receptors, support the second possibility. The results, however, do not exclude the possibility that intersynaptic diffusion of glutamate also has a role in the operation of the hippocampal network (Kullmann and Asztely, 1998). In any such scheme, however, it will be necessary to take into account the large variability in the AMPA receptor content of synapses and the existence of a large proportion of glutamatergic synapses with no or low numbers of AMPA receptors. As the size and geometry of the synapses vary greatly, the spatiotemporal profile of the transmitter will not be identical across synapses, which may effect the number and types of receptors contributing to the synaptic signal (Min et al., 1998). It has also been proposed that the transformation of synapses containing only NMDA receptors into AMPA/NMDA receptor–containing ones may underlie the expression of NMDA receptor–dependent long-term potentiation (LTP) (Kullmann, 1994; Isaac et al., 1995; Liao et al., 1995) and functional synapse formation during postnatal development (Durand et al., 1996; Wu et al., 1996; Isaac et al., 1997). The finding that the proportion of immunonegative spine synapses in stratum radiatum of a P17 rat is almost twice as high as that in adult rats is in line with these results. Clearly, the determination of the NMDA receptor distribution at hippocampal synapses and the monitring of activity-dependent changes in the number of synaptic AMPA and NMDA receptors will be necessary to evaluate further these issues.

Quantitative Distribution of AMPA Receptors Differs in Functionally Distinct Excitatory Synapses

Most nerve cells in the central nervous system receive glutamatergic inputs from several sources. One type of connection usually exhibits a large mean amplitude with small trial to trial variability, which may be the consequence of a large number of synaptic junctions with high transmitter release probability. Examples include retinal input to relay cells of the dorsal lateral geniculate nucleus (d-LGN; Paulsen et al., 1997, Soc. Neurosci., abstract), geniculate input to layer IV spiny stellate cells of the visual cortex (Stratford et al., 1996), and mossy fiber input to CA3 pyramidal neurons (Jonas et al., 1993). Another type of connection has a smaller mean amplitude and larger trial to trial variability, probably due to a smaller number of release sites and a lower transmitter release probability. Cortical input to relay cells in the d-LGN (Paulsen et al., 1997, Soc. Neurosci., abstract), intracortical connection to layer IV spiny stellate cells (Stratford et al., 1996), and connections between CA3 pyramidal neurons (Debanne et al., 1996) are examples of the latter type of connection. As the functional role of the distinct excitatory afferents to the same cell differs, their activation may result in postsynaptic responses with dissimilar properties. Indeed, the mossy fiber and C/A synapses on CA3 pyramidal cells have different functional properties, and our results reveal a difference in their AMPA receptor content. Interestingly, these two connections exhibit different forms of synaptic plasticity. The induction of LTP at C/A synapses requires the activation of the NMDA-type GluRs and a rise in postsynaptic Ca^{2+}, whereas LTP at mossy fiber synapses is independent of NMDA receptor activation but requires a rise in presynaptic Ca^{2+} (Nicoll and Malenka, 1995). Additional, qualitative differences in the AMPA receptor subunit composition of mossy versus C/A synapses may also exist, similar to those for the NMDA receptors. Recent studies indicated that the NMDA receptor subunit composition of C/A synapses includes NR1, NR2A, and NR2B but that of mossy fiber synapses is NR1/NR2A (Fritschy et al., 1998; Watanabe et al., 1998).

Both Schaffer collateral synapses on CA1 and C/A synapses on CA3 pyramidal cells exhibit NMDA receptor–dependent LTP (Bliss and Collingridge, 1993) and show a strongly skewed distribution of AMPA receptor content with large variability, including a significant proportion of synapses having an undetectable level of receptors. Such similar characteristics suggest that this pattern of AMPA receptor content may be a general feature of glutamatergic synapses that display NMDA receptor–dependent LTP. This notion is supported by the finding that GABAergic interneurons that do not show NMDA receptor–dependent LTP (Maccaferri and McBain, 1996; McMahon and Kauer, 1997) exhibit an AMPA receptor content very different from Schaffer collateral and C/A synapses but similar to that of mossy fiber synapses. The identification of distinct molecular fingerprints for these different types of connection will help us to predict the functional properties and the type of plasticity of other excitatory connections of the brain.

Heterogeneity of Schaffer Collateral Synapses on CA1 Pyramidal Cells

The very skewed distribution of spine synapses in the stratum radiatum indicates that these synapses do not form a homogeneous population with regard to their AMPA receptor content. In adult rats, ~15% of the synapses probably have less than 3 functional AMPA receptors (assuming a similar scaling factor in adult and P17 rats), the majority of the synapses (~65%) contain between 3 and 23 receptors, and ~20% of the spine synapses accommodate a large number of AMPA receptors (25–200). Heterogeneity of synapses according to their

AMPA/NMDA receptor content has also been suggested in cultured hippocampal neurons (Richmond et al., 1996; Rao et al., 1998). It is very likely that the distribution recorded at any one time is just a snapshot of a dynamically changing pattern. LTP-like processes may convert AMPA receptor–negative synapses into weakly positive ones and eventually strongly positive ones (reviewed by Ben-Ari et al., 1997; Malenka and Nicoll, 1997), if action potentials in the postsynaptic cell consistently occur shortly after the presynaptic release of transmitter (Markram et al., 1997; Debanne et al., 1998). The reverse process may also occur.

The efficacy of synaptic interaction between two nerve cells is not exclusively determined by the receptor content of synapses. Other factors such as the number of synaptic junctions between two cells, the transmitter release probability at each release site, the spatiotemporal profile of transmitter concentration in the cleft, and the properties of the receptors are also important. When connections between nerve cells are established, the interaction may be mediated by a single release site that originally does not contain AMPA receptors but at which receptors are inserted (Isaac et al., 1995; Liao et al., 1995; Durand et al., 1996) if the activity of pre- and postsynaptic cells temporarily coincides (Markram et al., 1997; Debanne et al., 1998). As more AMPA receptors are inserted into the synapse and the synaptic area also grows, the postsynaptic receptor occupancy may become sufficiently low (Silver et al., 1996; Forti et al., 1997; Nusser et al., 1997) that the further insertion of new receptors will not result in a significant increase in the postsynaptic response. At such connections, multiple synaptic contacts may be formed between the neurons (Bolshakov et al., 1997) if further increase in the synaptic efficacy is required. This would correspond to the late phase of synaptic plasticity, which is dependent on protein synthesis (Frey et al., 1988).

The question arises whether, in the fully formed functional system, a connection between two cells includes synapses either rich or poor in AMPA receptors. The number of synapses in unitary connections from CA3 to CA1 pyramidal cells has not been directly established, but depending on the preparation the predominance of both single release sites (Raastad et al., 1992; Stevens and Wang, 1994; Bolshakov and Siegelbaum, 1995) or multiple release sites (Malinow, 1991; Larkman et al., 1992) has been proposed. It is possible that functionally important, strong connections between pyramidal cells are mediated by multiple release sites, each having a large number of AMPA receptors. Long-term modifications of such connections may not involve synaptic insertion of new receptors but rather a redistribution of synaptic efficacy, as has been suggested to occur between layer 5 pyramidal cells in the neocortex (Markram and Tsodyks, 1996). The majority of connections between CA3 and CA1 pyramidal cells may be weak, mediated by a single release site with a relatively small quantal size (Stevens and Wang, 1994; Bolshakov and Siegelbaum, 1995) or without functional AMPA receptors (Isaac et al., 1995; Liao et al., 1995; Durand et al., 1996). When such weak connections become functionally relevant, both the recruitment of AMPA receptors to the single synaptic junction and the development of new synaptic sites may take place. These possibilities can be tested through paired recordings and combined high resolution anatomical analysis.

Synaptic Targeting of AMPA-Type GluRs

The details of how AMPA receptors are selectively targeted to glutamatergic synapses are poorly understood, but several mechanisms have been proposed (Craig et al., 1994; Steward, 1995; Kirsch et al., 1996; Richmond et al., 1996; Sheng, 1997). Receptors may be synthesized in the soma and transported to the synapse either within intracellular transport vesicles or by lateral transport in the plasma membrane. Alternatively, mRNAs for receptors may be transported to the synapse, and local protein synthesis could ensure the selective insertion of receptor proteins into the synaptic junction as it has been suggested for the glycine receptor α subunit (Racca et al., 1997). Depending on the transport mechanisms, receptors are expected to be present either in the extrasynaptic plasma membrane close to synapses or in intracellular membranes. Furthermore, if synaptic plasticity involves AMPA receptor insertion into the synaptic membrane, it necessitates the presence of an AMPA receptor pool close to the synapse, because LTP develops within minutes. Indeed, pharmacological interference with membrane fusion in the postsynaptic cell prevents LTP (Lledo et al., 1998). In the present study, we have described a significant pool of receptors associated with the spine apparatus and also confirmed the presence of immunoreactive AMPA receptors in the extrasynaptic spine membrane (Baude et al., 1995). However, very little immunoreactive receptor was observed in the spine apparatus and extrasynaptic plasma membrane of small spines that received an immunonegative or a weakly positive synapse. Although, the dendritic shaft at the origin of such spines has not been extensively studied, because it is almost always outside the section series of the spine head, an enrichment of AMPA receptors has not been found in the dendritic smooth or rough endoplasmic reticulum. A low level of labeling could be detected reliably in dendritic endoplasmic reticulum. A much larger pool of receptors in the spine apparatus and extrasynaptic plasma membrane positions was observed at large spines, which bore a strongly positive synapse. This observation supports the view that AMPA receptors in the spine apparatus and extrasynaptic plasma membrane locations represent receptors involved in receptor turnover, although they may also participate in synaptic plasticity.

Experimental Procedures

Preparation of Tissue

Four adult (three male and one female) rats (Wistar; ~150 g) and one P17 (male) rat (Wistar) were anesthetized with Sagatal (pentobarbitone sodium, 220 mg/kg intraperitoneally) and perfused through the heart with saline followed by fixative containing 4% paraformaldehyde, 0.025%–0.05% glutaraldehyde, and ~0.2% picric acid in 0.1 M phosphate buffer (PB; pH 7.4) for 15–25 min. After perfusion, the brains were removed, and blocks from the dorsal hippocampus were cut out and washed in several changes of PB. Freeze substitution and low temperature embedding in acrylic resins were carried out as described earlier (Baude et al., 1995; Nusser et al., 1997). For cryoprotection, sections (500 μm thickness, cut with a Vibratome) were placed either into 1 M sucrose solution in PB for

2 hr or in 10%, 20%, or 30% glycerol in 0.1 M Tris-maleate buffer (pH 7.4) overnight. They were then slammed onto copper blocks cooled in liquid N_2. This was followed by freeze-substitution with methanol and embedding either in Lowicryl HM 20 (Chemische Werke Lowi GMBH, Germany) or in Unicryl (BioCell International, Cardiff, United Kingdom) resins.

Antibodies

A polyclonal antibody to a C-terminal peptide common to the GluR2, GluR3, and GluR4c subunits of the AMPA-type GluR was used at the final protein concentration of 1–1.7 μg/ml. The characterization of antibody GluR2/3/4c has been described earlier (Wenthold et al., 1992). We refer to this antibody as recognizing the GluR2/3 subunits (ab-GluR2/3).

Production and Characterization of the pan-AMPA Antibody

Expression and Purification of Glutathione S-Transferase–GluR1$_{flop}$ Fusion Proteins

Glutathione S-transferase (GST) fusion proteins containing 58 amino acid residues preceding the last membrane-spanning segment of GluR1$_{flop}$ (Hollmann et al., 1989) were produced. A DNA fragment encoding amino acid residues 724–781 of GluR1$_{flop}$ was synthesized by polymerase chain reaction (PCR). Products were purified on a 10% acrylamide gel, digested with BamHI and HindIII, purified again on a 10% acrylamide gel, and ligated into a BamHI- and HindIII-digested pGEX-2TH bacterial expression vector (Pharmacia). For expression of GST fusion proteins, *Escherichia coli* strain HB101 competent cells (Promega) were transformed with the vector and grown in 2-YT medium containing 0.2% glucose and 50 μg/ml ampicillin. Expression of recombinant protein was induced by addition of 1 mM isopropyl-1-thio-β-D-galactopyranoside. The fusion protein was extracted and was loaded onto a glutathione agarose column for purification. Purified proteins were analyzed by sodium dodecyl sulphate–polyacrylamide gel electrophoresis (SDS-PAGE) on a 15% gel, and the protein concentration was determined.

Generation and Purification of Antibodies

Four rabbits were subcutaneously injected with the purified GST–GluR1$_{flop}$ fusion proteins (0.5 mg), boosted every 4 weeks, and bled 10 days after each boost. The antisera were preadsorbed using a Sepharose 4B column coupled with the unfused GST protein. Subsequently, GluR1 portion–specific antisera were affinity purified with a Sepharose 4B column coupled with the GST fusion protein containing residues 724–781. The antibodies were eluted with a buffer containing 0.1 M glycine-HCl (pH 2.5) and immediately neutralized with 1/10 volume of 1 M Tris-base (pH 8.0). The antibody solution was dialyzed three times against a 1000-fold volume of phosphate-buffered saline (PBS). All rabbits immunized produced antibodies recognizing the fusion proteins. For postembedding reactions, affinity-purified pan-AMPA3/3 (rabbit 3, bleed 3) was used at a final protein concentration of 7.5–15 μg/ml.

Preparation of Membrane Fractions, SDS-PAGE, and Immunoblot Analysis

The culturing of COS7 cells, the transient transfection with cDNA coding for different GluR subunits, the membrane preparation from transfected cells and from adult rat brains, and SDS-PAGE were performed as described previously (Molnar et al., 1993; McIlhinney and Molnar, 1996). For immunoblot, affinity-purified ab-pan-AMPA was used at a final protein concentration of 1 μg/ml (12–16 hr incubation at 4°C). The bound antibodies were detected with peroxidase-conjugated anti-rabbit IgG secondary antibody using enhanced chemiluminescence (ECL; Pierce, Rockford, IL). The pan-AMPA antibody specifically recognized GST fusion proteins incorporating residues 724–781, whereas GST alone was not recognized. In immunoblot experiments using membrane extracts from cell lines expressing different GluR subunits, the antibodies strongly labeled AMPA receptor subunits GluR1–GluR4 but not kainate receptor subunits GluR5–GluR7 (Figure 1). Using membranes from rat whole brain, the affinity purified pan-AMPA antibody recognized a single band at ~110 kDa. Furthermore, the pan-AMPA polyclonal antibody cross-reacts with both "flip" and "flop" splice variants with about equal intensity.

Postembedding Immunocytochemistry and Controls

Two different methods were applied.

First, Lowicryl or Unicryl resin–embedded ultrathin sections (70–80 nm thickness) were picked up on pioloform-coated nickel slot grids and were incubated on drops of blocking solution (50 mM Tris-HCl [pH 7.4] containing 0.3% NaCl [TBS] and 5%–20% normal goat serum) for 30 min. This was followed by an incubation on drops of primary antibodies (diluted in TBS containing 2% normal goat serum) overnight (Baude et al., 1995). In some reactions, the blocking and the primary antibody solutions contained 0.03% Triton X-100. Second, reactions were carried out on 70–90 nm thick sections of Lowicryl resin–embedded hippocampal tissue. The sections were picked up either on 400 mesh gold grids or on pioloform-coated nickel slot grids. The sections were then treated with a saturated solution of NaOH in 100% ethanol for 1–3 s. After washing, the sections were incubated in TBS containing 0.1% Triton X-100 (TBST) and 0.1% sodium borohydride and 50 mM glycine for 10 min. Human serum albumin (HSA; 2% in TBST) was used for blocking for 30 min, followed by an incubation with the primary antibodies (diluted in TBST containing 2% HSA) overnight (Matsubara et al., 1996).

After the incubation in primary antibodies, the sections were washed and incubated on drops of goat anti-rabbit IgG coupled to 10 nm gold particles (diluted 1:100; Nanoprobes, Stony Brook, NY or BioCell International) for 2 hr at room temperature. After further washing in ultra-pure water, the sections were contrasted with saturated aqueous uranyl acetate followed by staining with lead citrate. Selective labeling, resembling that obtained with the specific antibodies, could not be detected when the primary antibodies were either omitted or replaced by 5% normal rabbit serum.

Quantification of Immunoreactivity

Serial ultrathin sections (12–35/grid) were cut from the CA1 or CA3 regions of the hippocampus, and each section was reacted for AMPA-type GluR subunits.

Areas in the stratum radiatum of the CA1 and CA3 regions were randomly chosen and were photographed in 12–35 serial sections and printed at a magnification of 32,000×–42,000×. Synapses made by axon terminals with pyramidal cell spines and with interneuron dendrites were only included in the analysis if they were fully present within the serially sectioned volume of tissue. A dendrite was classified as belonging to an interneuron if it received several asymmetrical synapses on its shaft and did not emit spines.

Areas in the stratum lucidum of the CA3 region were randomly photographed and followed through 25–35 serial sections, and every complete synaptic specialization made by large mossy fiber terminals with pyramidal cell complex spines was analyzed individually. Mossy fiber terminals were recognized from their ultrastructural characteristics: large size, large number of synaptic vesicles, clusters of mitochondria, and, often, the presence of numerous dense-core vesicles.

Immunoparticles were counted within the anatomically defined synaptic junctions. The length of the junction was also measured on each ultrathin section. The synaptic area was calculated by multiplying the synaptic length in each section with the estimated thickness of the electron microscopic section (e.g., 75 nm); areas were then summed from all sections through each synapse.

Each block of tissue of the CA3 region contained both strata radiatum and lucidum; thus, the three synapse populations in the CA3 area (spines in the radiatum, interneuron dendritic shafts, and mossy fiber terminals to spines) originate from the same reaction, making quantitative comparisons possible. However, the measurements of synapses in the CA1 area originate from different blocks and reactions from those obtained in the CA3 area. Therefore, comparison between the CA1 and CA3 areas can be made only after normalization.

Acknowledgments

The authors are grateful to Dr. Ryuichi Shigemoto for his advice on selecting the epitope and producing the fusion protein for ab-pan-AMPA, to Miss Zahida Ahmad for excellent technical assistance, and to Mr. Paul Jays for photographic assistance. We would like to thank Drs. Claudia Racca, Istvan Mody, and Ole Paulsen for their comments on the manuscript. We are also grateful to Dr. Robert J. Wenthold for kindly providing the ab-GluR2/3. This study was supported by the Medical Research Council (United Kingdom) and a

European Commission Shared Cost RTD Programme Grant (number BIO4CT96–0585).

Received April 27, 1998; revised July 21, 1998.

References

Andersen, P., Blackstad, T.W., and Lomo, T. (1966). Location and identification of excitatory synapses on hippocampal pyramidal cells. Exp. Brain Res. *1*, 236–248.

Baude, A., Molnar, E., Latawiec, D., McIlhinney, R.A.J., and Somogyi, P. (1994). Synaptic and nonsynaptic localization of the GluR1 subunit of the AMPA-type excitatory amino acid receptor in the rat cerebellum. J. Neurosci. *14*, 2830–2843.

Baude, A., Nusser, Z., Molnar, E., McIlhinney, R.A.J., and Somogyi, P. (1995). High-resolution immunogold localization of AMPA type glutamate receptor subunits at synaptic and non-synaptic sites in rat hippocampus. Neuroscience *69*, 1031–1055.

Ben-Ari, Y., Khazipov, R., Leinekugel, X., Caillard, O., and Gaiarsa, J.L. (1997). $GABA_A$, NMDA and AMPA receptors: a developmentally regulated "menage a trois." Trends Neurosci. *20*, 523–529.

Bliss, T.V.P., and Collingridge, G.L. (1993). A synaptic model of memory: long-term potentiation in the hippocampus. Nature *361*, 31–39.

Bolshakov, V.Y., and Siegelbaum, S.A. (1995). Regulation of hippocampal transmitter release during development and long-term potentiation. Science *269*, 1730–1734.

Bolshakov, V.Y., Golan, H., Kandel, E.R., and Siegelbaum, S.A. (1997). Recruitment of new sites of synaptic transmission during the cAMP-dependent late phase of LTP at CA3–CA1 synapses in the hippocampus. Neuron *19*, 635–651.

Chicurel, M.E., and Harris, K.M. (1992). Three-dimensional analysis of the structure and composition of CA3 branched dendritic spines and their synaptic relationships with mossy fiber boutons in the rat hippocampus. J. Comp. Neurol. *325*, 169–182.

Craig, A.M., Blackstone, C.D., Huganir, R.L., and Banker, G. (1994). Selective clustering of glutamate and γ-aminobutyric acid receptors opposite terminals releasing the corresponding neurotransmitters. Proc. Natl. Acad. Sci. USA *91*, 12373–12377.

Debanne, D., Guerineau, N.C., Gahwiler, B.H., and Thompson, S.M. (1996). Paired-pulse facilitation and depression at unitary synapses in rat hippocampus: quantal fluctuation affects subsequent release. J. Physiol. (Lond.) *491*, 163–176.

Debanne, D., Gahwiler, B.H., and Thompson, S.M. (1998). Long-term plasticity between pairs of individual CA3 pyramidal cells in rat hippocampal slice cultures. J. Physiol. (Lond.) *507*, 237–247.

Dobrunz, L.E., and Stevens, C.F. (1997). Heterogeneity of release probability, facilitation, and depletion at central synapses. Neuron *18*, 995–1008.

Durand, G.M., Kovalchuk, Y., and Konnerth, A. (1996). Long-term potentiation and functional synapse induction in developing hippocampus. Nature *381*, 71–75.

Forti, L., Bossi, M., Bergamaschi, A., Villa, A., and Malgaroli, A. (1997). Loose-patch recordings of single quanta at individual hippocampal synapses. Nature *388*, 874–878.

Frey, U., Krug, M., Reymann, K.G., and Matties, H. (1988). Anisomycine, an inhibitor of protein synthesis, blocks late phases of LTP phenomena in the hippocampal CA1 region in vitro. Brain Res. *452*, 57–65.

Fritschy, J.-M., Weinmann, O., Wenzel, A., and Benke, D. (1998). Synapse-specific localization of NMDA and $GABA_A$ receptor subunits revealed by antigen-retrieval immunohistochemistry. J. Comp. Neurol. *390*, 194–210.

Harris, K.M., and Kater, S.B. (1994). Dendritic spines: cellular specializations imparting both stability and flexibility to synaptic function. Annu. Rev. Neurosci. *17*, 341–371.

Hollmann, M., O'Shea-Greenfield, A., Rogers, S.W., and Heinemann, S. (1989). Cloning by functional expression of a member of the glutamate receptor family. Nature *342*, 643–648.

Isaac, J.T.R., Nicoll, R.A., and Malenka, R.C. (1995). Evidence for silent synapses: implications for the expression of LTP. Neuron *15*, 427–434.

Isaac, J.T.R., Crair, M.C., Nicoll, R.A., and Malenka, R.C. (1997). Silent synapses during development of thalamocortical inputs. Neuron *18*, 269–280.

Jack, J.J.B., Larkman, A.U., Major, G., and Stratford, K.J. (1994). Quantal analysis of the synaptic excitation of CA1 hippocampal pyramidal cells. In Molecular and Cellular Mechanisms of Neurotransmitter Release, L. Stjarne, P. Greengard, S. Grillner, T. Hokfelt, and D. Ottoson, eds. (New York: Raven Press), pp. 275–299.

Jonas, P., Major, G., and Sakmann, B. (1993). Quantal components of unitary EPSCs at the mossy fibre synapse on CA3 pyramidal cells of rat hippocampus. J. Physiol. (Lond.) *472*, 615–663.

Kharazia, V.N., Wenthold, R.J., and Weinberg, R.J. (1996). GluR1-immunopositive interneurons in rat neocortex. J. Comp. Neurol. *368*, 399–412.

Kirsch, J., Meyer, G., and Betz, H. (1996). Synaptic targeting of ionotropic neurotransmitter receptors. Mol. Cell. Neurosci. *8*, 93–98.

Kullmann, D.M. (1994). Amplitude fluctuations of dual-component EPSCs in hippocampal pyramidal cells: implications for long-term potentiation. Neuron *12*, 1111–1120.

Kullmann, D.M., and Asztely, F. (1998). Extrasynaptic glutamate spillover in the hippocampus: evidence and implications. Trends Neurosci. *21*, 8–14.

Kullmann, D.M., Erdemli, G., and Asztely, F. (1996). LTP of AMPA and NMDA receptor–mediated signals: evidence for presynaptic expression and extrasynaptic glutamate spill-over. Neuron *17*, 461–474.

Landsent, A.S., Amiri-Moghaddam, M., Matsubara, A., Bergensen, L., Usami, S., Wenthold, R.J., and Ottersen, O.P. (1997). Differential localization of δ glutamate receptors in the rat cerebellum: coexpression with AMPA receptors in parallel fiber–spine synapses and absence from climbing fiber–spine synapses. J. Neurosci. *17*, 834–842.

Larkman, A., Hannay, T., Stratford, K., and Jack, J. (1992). Presynaptic release probability influences the locus of long-term potentiation. Nature *360*, 70–73.

Liao, D., Hessler, N.A., and Malinow, R. (1995). Activation of postsynaptically silent synapses during pairing-induced LTP in CA1 region of hippocampal slice. Nature *375*, 400–404.

Lledo, P.-M., Zhang, X., Sudhof, T.C., Malenka, R.C., and Nicoll, R.A. (1998). Postsynaptic membrane fusion and long-term potentiation. Science *279*, 399–403.

Maccaferri, G., and McBain, C.J. (1996). Long-term potentiation in distinct subtypes of hippocampal nonpyramidal neurons. J. Neurosci. *16*, 5334–5343.

Malenka, R.C., and Nicoll, R.A. (1997). Silent synapses speak up. Neuron *19*, 473–476.

Malinow, R. (1991). Transmission between pairs of hippocampal slice neurons: quantal levels, oscillations, and LTP. Science *252*, 722–724.

Markram, H., and Tsodyks, M. (1996). Redistribution of synaptic efficacy between neocortical pyramidal neurons. Nature *382*, 807–810.

Markram, H., Lubke, J., Frotscher, M., and Sakmann, B. (1997). Regulation of synaptic efficacy by coincidence of postsynaptic APs and EPSPs. Science *275*, 213–215.

Martin, L.J., Blackstone, C.D., Levey, A.I., Huganir, R.L., and Price, D.L. (1993). AMPA glutamate receptor subunits are differentially distributed in rat brain. Neuroscience *53*, 327–358.

Matsubara, A., Laake, J.H., Davanger, S., Usami, S., and Ottersen, O.P. (1996). Organization of AMPA receptor subunits at a glutamate synapse: a quantitative immunogold analysis of hair cell synapses in the rat organ of Corti. J. Neurosci. *16*, 4457–4467.

McIlhinney, R.A.J., and Molnar, E. (1996). Characterization, cell-surface expression and ligand-binding properties of different truncated N-terminal extracellular domains of the ionotropic glutamate receptor subunit GluR1. Biochem. J. *315*, 217–225.

McMahon, L.L., and Kauer, J.A. (1997). Hippocampal interneurons express a novel form of synaptic plasticity. Neuron *18*, 295–305.

Min, M.-Y., Rusakov, D.A., and Kullmann, D.M. (1998). Activation of AMPA, kainate, and metabotropic receptors at hippocampal mossy fiber synapses: role of glutamate diffusion. Neuron *21*, this issue, 561–571.

Molnar, E., Baude, A., Richmond, S.A., Patel, P.B., Somogyi, P., and McIlhinney, R.A.J. (1993). Biochemical and immunocytochemical characterization of antipeptide antibodies to a cloned GluR1 glutamate receptor subunit: cellular and subcellular distribution in the rat forebrain. Neuroscience *53*, 307–326.

Moser, M.-B., Trommald, M., Egeland, T., and Andersen, P. (1997). Spatial training in a complex environment and isolation alter the spine distribution differently in rat CA1 pyramidal cells. J. Comp. Neurol. *380*, 373–381.

Nicoll, R.A., and Malenka, R.C. (1995). Contrasting properties of two forms of long-term potentiation in the hippocampus. Nature *377*, 115–118.

Nusser, Z., Mulvihill, E., Streit, P., and Somogyi, P. (1994). Subsynaptic segregation of metabotropic and ionotropic glutamate receptors as revealed by immunogold localization. Neuroscience *61*, 421–427.

Nusser, Z., Sieghart, W., Benke, D., Fritschy, J.-M., and Somogyi, P. (1996). Differential synaptic localization of two major γ-aminobutyric acid type A receptor α subunits on hippocampal pyramidal cells. Proc. Natl. Acad. Sci. USA *93*, 11939–11944.

Nusser, Z., Cull-Candy, S.G., and Farrant, M. (1997). Differences in synaptic $GABA_A$ receptor number underlie variation in GABA mini amplitude. Neuron *19*, 697–709.

Petralia, R.S., and Wenthold, R.J. (1992). Light and electron immunocytochemical localization of AMPA-selective glutamate receptors in the rat brain. J. Comp. Neurol. *318*, 329–354.

Popratiloff, A., Weinberg, R.J., and Rustioni, A. (1996). AMPA receptor subunits underlying terminals of fine-caliber primary afferent fibers. J. Neurosci. *16*, 3363–3372.

Raastad, M., Storm, J.F., and Andersen, P. (1992). Putative single quantum and single fibre excitatory postsynaptic currents show similar amplitude range and variability in rat hippocampal slices. Eur. J. Neurosci. *4*, 113–117.

Racca, C., Gardiol, A., and Triller, A. (1997). Dendritic and postsynaptic localizations of glycine receptor α subunit mRNAs. J. Neurosci. *17*, 1691–1700.

Rao, A., Kim, E., Sheng, M., and Craig, A.M. (1998). Heterogeneity in the molecular composition of excitatory postsynaptic sites during development of hippocampal neurons in culture. J. Neurosci. *18*, 1217–1229.

Richmond, S.A., Irving, A.J., Molnar, E., McIlhinney, R.A.J., Michelangeli, F., Henley, J.M., and Collingridge, G.L. (1996). Localization of the glutamate receptor subunit GluR1 on the surface of living and within cultured hippocampal neurons. Neuroscience *75*, 69–82.

Rogers, S.W., Hughes, T.E., Hollmann, M., Gasic, G.P., Deneris, E.S., and Heinemann, S. (1991). The characterization and localization of the glutamate receptor subunit GluR1 in the rat brain. J. Neurosci. *11*, 2713–2724.

Rubio, M.E., and Wenthold, R.J. (1997). Glutamate receptors are selectively targeted to postsynaptic sites in neurons. Neuron *18*, 939–950.

Sato, K., Kiyama, H., and Tohyama, M. (1993). The differential expression patterns of messenger RNAs encoding non-N-methyl-D-aspartate receptor subunits (GluR1–4) in the rat brain. Neuroscience *52*, 515–539.

Schikorski, T., and Stevens, C.F. (1997). Quantitative ultrastructural analysis of hippocampal excitatory synapses. J. Neurosci. *17*, 5858–5867.

Sheng, M. (1997). Glutamate receptors put in their place. Nature *386*, 221–223.

Shigemoto, R., Kulik, A., Roberts, J.D.B., Ohishi, H., Nusser, Z., Kaneko, T., and Somogyi, P. (1996). Target-cell-specific concentration of a metabotropic glutamate receptor in the presynaptic active zone. Nature *381*, 523–525.

Silver, R.A., Cull-Candy, S.G., and Takahashi, T. (1996). Non-NMDA glutamate receptor occupancy and open probability at a rat cerebellar synapse with single and multiple release sites. J. Physiol. (Lond.) *494*, 231–250.

Sommer, B., Keinanen, K., Verdoorn, T.A., Wisden, W., Burnashev, N., Herb, A., Kohler, M., Takagi, T., Sakmann, B., and Seeburg, P.H. (1990). Flip and flop: a cell-specific functional switch in glutamate-operated channels of the CNS. Science *249*, 1580–1585.

Sorra, K.E., and Harris, K.M. (1998). Stability in synapse number and size at 2 hr after long-term potentiation in hippocampal area CA1. J. Neurosci. *18*, 658–671.

Stevens, C.F., and Wang, Y. (1994). Changes in reliability of synaptic function as a mechanism for plasticity. Nature *371*, 704–707.

Steward, O. (1995). Targeting of mRNAs to subsynaptic microdomains in dendrites. Curr. Opin. Neurobiol. *5*, 55–61.

Stratford, K.J., Tarczy-Hornoch, K., Martin, K.A.C., Bannister, N.J., and Jack, J.J.B. (1996). Excitatory synaptic inputs to spiny stellate cells in cat visual cortex. Nature *382*, 258–261.

Watanabe, M., Fukaya, M., Sakimura, K., Manabe, T., Mishina, M., and Inoue, Y. (1998). Selective scarcity of NMDA receptor channel subunits in the stratum lucidum (mossy fibre recipient layer) of the mouse hippocampal CA3 subfield. Eur. J. Neurosci. *10*, 478–487.

Wenthold, R.J., Yokotani, N., Doi, K., and Wada, K. (1992). Immunochemical characterization of the non-NMDA glutamate receptor using subunit-specific antibodies. J. Biol. Chem. *267*, 501–507.

Wu, G.-Y., Malinow, R., and Cline, H.T. (1996). Maturation of a central glutamatergic synapse. Science *274*, 972–976.